Theory of polaron resonance in quantum dots and quantum-dot molecules

K.-M. Hung[a)]
Department of Electronics Engineering, National Kaohsiung University of Applied Sciences, Kaohsiung, Taiwan 807, Republic of China

(Received 22 March 2007; accepted 4 June 2007; published online 31 July 2007)

This work presents the theory of exciton coupling to photons and longitudinal optical (LO) phonons in quantum dots (QDs) and quantum-dot molecules (QDMs). Resonant-round trips of the exciton between the ground (bright) and excited (dark or bright) states, mediated by the LO phonon, alter the decay time and yield the Rabi oscillation. The initial distributions of the population in the ground and the excited states dominate the oscillating amplitude and frequency. This property provides a detectable signature to the information that is stored in a qubit that is made from QD or QDM, over a wide range of temperatures *T*. The results herein explain the anomaly of *T*-dependent decay in self-assembled InGaAs/GaAs QDMs, which has recently been experimentally identified. © *2007 American Institute of Physics*. [DOI: 10.1063/1.2756621]

I. INTRODUCTION

Charge carriers that move in semiconductor quantum dots (QDs) and quantum-dot molecules (QDMs) provide a larger transition-dipole moment than that in atomic and molecular systems, owing to the interaction with solid-state matter and a spatial variation of the band edge in QDs and QDMs. This fact supports applications in quantum information processing[1] and logical operation.[2,3] In such applications, the coherent manipulation of the excitonic wave function in QDs and QDMs at finite temperature is essential. The dephasing time [~1 ns in self-assembled InGaAs/GaAs QDs (Refs. 4–6) and QDMs (Refs. 6 and 7)] must be longer than the manipulation time (~1 ps),[8] because the coherence of the excitonic transition, or quantum computation, cannot be maintained when the dephasing time is similar to or less than the manipulation time.

In QD and QDM systems, carrier dephasing can be categorized into two parts; (1) the dephasing of the spatial wave function of the exciton and (2) the dephasing of the internal degrees of freedom of the exciton, such as degenerate spin states. The former dephasing is mainly attributed to, for example, photon and real phonon scattering, as in the so-called excitonic decay, because the exciton cannot incoherently reside in a spatially confined state. The second dephasing relaxes the internal degrees of freedom of the exciton from one of its degenerate states to the others, or changes the phase relation of the state that is a superposition of degenerate states, while preserving spatial coherence; it thus conserves the number of excitons, as in so-called pure dephasing. In fact, pure dephasing can also affect the decay time through, for example, the relaxation between spin-dark and spin-bright states according to the selection rule of photon emission.[6] Recently, both experimental and theoretical investigations[9,10] have revealed that the virtual-phonon processes for both acoustic and optical phonons result in second dephasing and exhibit a nonmonotonous *T* dependence in rapid initial decoherence (~1 ps).[11]

In principle, the charge cancellation of the identical distributions of electrons and holes in a strongly confining QD reduces the interaction of excitons with longitudinal optical (LO) phonons,[12–14] and a large level spacing reduces the strength of exciton scattering from real acoustic phonons. Accordingly, a long decay is expected. However, the presence of piezoelectric fields,[15] fluctuations in the shape and/or the size of QDs,[16] the Jahn–Teller effect,[17] and charged point defects[18] lead to polarization of the charge distributions, which strengthens LO phonon-exciton coupling. For the electronic polaron,[19] coherent interactions of the electron-hole pair with a polarizable field (a real optical phonon) form an excitonic polaron and do not contribute to phase decoherence, because the dressed state is an eigenvector of the interacting exciton-LO-phonon system. The resonance of an excitonic polaron has been demonstrated experimentally to exist when an energy separation between the electronic states approaches one or several LO-phonon energies.[20] Such resonance is hard to occur in bulk, quantum well or quantum wire structures, according to the phase decoherence through the process of real acoustic phonon, which is strongly suppressed in QDs and QDMs by the large spacing between levels.

The decay may result from the emission of a photon, the coupling of the phonon thermostat that originates in the anharmonicity of the crystal,[19] the thermal emission of carriers from the dots at high temperature *T* (Ref. 6), and virtual phonon processes.[9–11] When the second effect is neglected, the delta-like density of states of QD prevents *k*-space thermalization, resulting in a nearly constant decay time with respect to *T* in situations in which thermal emission can be ignored and the time scale is far from that of the pure dephasing, because the photon emission is independent of *T*. Yet, this feature differs dramatically in self-assembled InGaAs/GaAs QDs (Ref. 21) and QDMs,[6] for which the decay time increases with *T*. This feature cannot be described as the thermal recycling of the carriers[6,22] because it almost disappears in the InGaAs/GaAs QDs with the same structure as used in the QDMs.[6] Instead, the thermal population of

[a)]Electronic mail: kmhung@cc.kuas.edu.tw

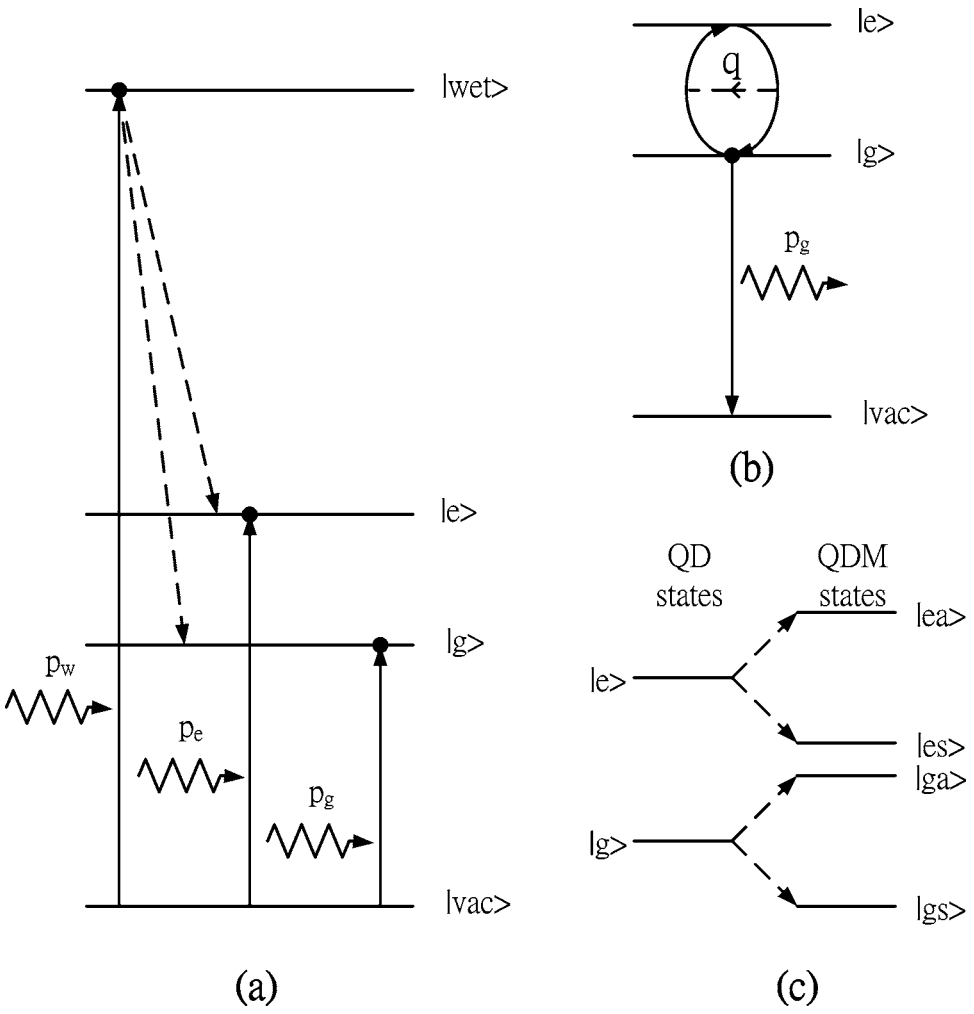

FIG. 1. (a) Schematic excitation processes. (b) Three-level excitonic system for QD or QDM; solid-wiggled (dashed) lines denote photon (phonon) absorption/emission. (c) Schematic splitting of QD states into symmetric ($|gs\rangle$ and $|es\rangle$, bright) states and antisymmetric ($|ga\rangle$ and $|ea\rangle$, dark) states for QDM.

optically inactive states offers a reasonable explanation of the increase in the decay time as with lattice temperature.

This work presents a theory of the coupling of excitons to photons and LO phonons that are associated with dark or weak-bright excited states to explain the anomaly.[6] The theoretical results also reveal the time-dependent Rabi oscillation (RO) for both QD and QDM systems.[23] The oscillating frequency and the oscillating amplitude of the ROs depend strongly on the initial distributions of the excitonic population, which depend on the manner of excitation, as presented in Fig. 1(a). This property provides a detectable signature to the information that is stored in a qubit that is made from QD or QDM, with a long lifetime over a wide range of temperatures.

Section II presents a simple model of exciton coupling to photons and LO phonons and its corresponding Hamiltonian. Based on the Hamiltonian, Sec. III derives the dynamics of the exciton population in QDs/QDMs. Section IV presents and discusses the numerical results concerning the T-dependent decay of an exciton in QD and QDM systems. Finally, Sec. V draws conclusions.

II. MODEL AND HAMILTONIAN

A. Physical picture and model

The basic concept of the proposed theory can be understood as follows. Consider a three-level system of a QD or QDM that is embedded in a phonon bath, as displayed schematically in Fig. 1(b). The ground (bright) state $|g\rangle$ of the exciton is coupled to its vacuum state $|\text{vac}\rangle$ via the emission/absorption of a photon and coupled to the lowest excited state $|e\rangle$ by LO-phonon emission/absorption. The excited state can be a dark (or a weak bright) state in QDMs because of the symmetric and antisymmetric splitting in a symmetric structure[3] (or the interdot exciton for an asymmetric one) but a bright state in QDs, as shown in Fig. 1(c). A study of exciton-enhanced Raman scattering in bulk semiconductors proposed the same hypothesis.[24]

The effect of the brightness of the excited state, associated with the phonon-assisted transition, on the decay time of an exciton in QDs/QDMs is understood as follows. Imagine an hourglass with a controlled gate at the vent to control the rate of flow of sand (analogous to the optical-transition rate of an exciton). The hourglass has two positions—upstairs (state $|e\rangle$) and downstairs (state $|g\rangle$). The gate is assumed to be position-dependent—open (a bright exciton) downstairs with a flow (optical transition) rate of Γ_g, and open (bright exciton) or closed (dark or weak-bright exciton) upstairs with a rate Γ_e that depends on the system. The hourglass can be moved up and down between downstairs and upstairs (analogous to the RO of an exciton). The dynamics of the hourglass depend on the external force (temperature) that moves the hourglass to up and down between downstairs and

upstairs and on its transition rate γ_0 (which is analogous to the total coupling strength between the exciton and the LO phonon). When the hourglass remains downstairs (analogous to the absence of phonon-assisted transition at low T), the discharge time of the sand (the decay time of the exciton) is determined solely by the flow rate Γ_g.[25] When the hourglass moves up and down between upstairs and downstairs (such that RO is present), the discharge time will be governed by the flow rates associated with both upstairs and downstairs and by the dynamical distribution of the hourglass. In the (high T) case in which the hourglass is downstairs for half of the time and upstairs for the other half of the time, with an equal probability of moving up and down, the average flow rate is $(\Gamma_g+\Gamma_e)/2$. For $\Gamma_e=0$ or $\Gamma_e \ll \Gamma_g$ (a fully dark or weak-bright excited state), it is $\Gamma_g/2$ or double the discharge (decay) time. Hence, a fully dark-excited state maximally enhances the decay time, by a factor of 2. At moderate temperature, the average rate has the form $\sim N_{gNRO}(0^+)\Gamma_g + N_{eNRO}(0^+)\Gamma_e$, where N_{gNRO} (N_{eNRO}) denotes the initial number of excitons in state $|g\rangle$ ($|e\rangle$) with RO removed.

Although this model is simple, it sufficiently describes the mechanism of exciton decay by the interaction of excitons and LO phonons. Spontaneous emission of a LO phonon by an excited exciton, which is absent when the exciton is initially in its ground state, makes the T-dependent behavior of the exciton very sensitive to its initial population distribution.

B. Sudden approximation

Two experimental excitation approaches, schematically plotted in Fig. 1(a), provide low excitation power to prevent the effects of a charged exciton or biexciton that are frequently used in photoluminescence (PL) experiments. The first is (i) indirect excitation—in which excitons are initially created on the substrate or wetting layer and then relaxed into the states of QDs or QDMs. In such an excitation, a nonzero distribution of the exciton population in both the states $|g\rangle$ and $|e\rangle$ is possible. The second is (ii) direct excitation—in which the distribution of the excitonic population is initially determined from the frequency of the excitation light source. The rise time of the number of excitons depends on the mechanisms of carrier relaxation, optical transition, and excitation power, as well as on the duration of the excitation pulse.

A discussion of the rise time which is, in most cases, much shorter than the decay time, is beyond the scope of this work. The system is assumed promptly to respond to an ultrashort pulse excitation, in what is called the "sudden approximation" to avoid the complicated processes of exciton generation and rapid initial decay. In this approximation, the exciton abruptly appears in the system at time 0^+, before which time no transitions that would be caused by exciton-phonon and exciton-photon interactions occurs.[26] Although the sudden approximation does not apply to a real system, it is a good approximation when the decay time is much longer than the rise time, such as for exciton decay in InAs/GaAs QDs/QDMs.[6] It is also useful in simplifying theoretical derivation.

C. Hamiltonian

In the boson approximation, the interacting Hamiltonian of exciton coupling to photons and LO phonons (Fröhlich type) in a three-level system can be expressed as

$$H_I = \sum_p (\gamma_{pg}\hat{a}_p^+\hat{\alpha}_g + \text{c.c.}) + \sum_p (\gamma_{pe}\hat{a}_p^+\hat{\alpha}_e + \text{c.c.}) + \sum_q (\gamma_q \hat{d}_q^+\hat{\alpha}_g^+\hat{\alpha}_e + \text{c.c.}), \quad (1)$$

where $\hat{a}_p^+$ ($\hat{a}_p$), $\hat{d}_q^+$ ($\hat{d}_q$), and $\hat{\alpha}_i^+$ ($\hat{\alpha}_i$) are the creation (annihilation) operators of the photon, the LO phonon, and the exciton, respectively; γ_q (γ_{pi}) is the strength of coupling of the exciton to the LO phonons (photons). A rotationless approximation to the photon field is made, because the transition between spin-bright and spin-dark is not a major concern in this work. Notably, the exciton operators that are utilized in the pairing theory of superconductors[27] satisfy the algebra

$$[\hat{\alpha}_i, \hat{\alpha}_j^+] = \delta_{i,j}(1 - \hat{n}_{ei} - \hat{n}_{hi}), \quad (2)$$

because of the Pauli principle, where $\hat{n}_{e(h)i}$ is the number operator of electron (hole) in the state i. Although Eq. (2) is not in the form that is required by Bose–Einstein statistics, the factor $\hat{n}_{ei}+\hat{n}_{hi}$ does not affect the physics of the dynamics of the exciton when all orders of the resonant LO phonon are considered [with the phonon's momentum in the exciton loop conserved as displayed in Fig. 1(b), and detailed in Sec. III E] and in the second-order approximation to the photon correction. The definition of the exciton operator $\hat{\alpha}_i$, a product of the annihilation operators of the electron ($\hat{c}_i$) and the hole ($\hat{h}_i$) in the state i, gives the identities that are useful in the derivations of the equations of motion (EOM) of the exciton

$$\hat{\alpha}_i\hat{\alpha}_i = \hat{\alpha}_i^+\hat{\alpha}_i^+ = \hat{\alpha}_i^+\hat{n}_{ei} = \hat{\alpha}_i^+\hat{n}_{hi} = \hat{n}_{ei}\hat{\alpha}_i = \hat{n}_{hi}\hat{\alpha}_i = 0,$$

$$[\hat{\alpha}_i, \hat{n}_{ei}] = [\hat{\alpha}_i, \hat{n}_{hi}] = \hat{\alpha}_i, \quad (3)$$

$$[\hat{\alpha}_i^+, \hat{n}_{ei}] = [\hat{\alpha}_i^+, \hat{n}_{hi}] = -\hat{\alpha}_i^+.$$

D. Coupling strengths of photons

In the dipole approximation,[28] the coupling strength of the exciton to the photon has the form

$$\gamma_{pi} = i\frac{eE_i}{\hbar}\sqrt{\frac{2\pi\hbar}{\varepsilon_r\omega_p V}}\boldsymbol{\varepsilon}\cdot\langle\phi_i(r)|\mathbf{r}|\phi_i(r)\rangle, \quad (4)$$

where E_i and $\phi_i(r)$ are the exciton energies of the state i and its associated wave function (in relative coordinate), respectively; $\boldsymbol{\varepsilon}$ is the polarization vector of the photon field; ω_p is the photon frequency of mode p; e is the bare electron charge, and ε_r is the relative dielectric constant of the material of the dot. The coupling strength, Eq. (4), gives the emission rate[28]

$$2\Gamma_i = \frac{4}{3}\frac{e^2\omega_i^3}{\varepsilon_r \hbar c^3}|\langle\phi_i|\mathbf{r}|\phi_i\rangle|^2, \tag{5}$$

where $\omega_i = E_i/\hbar$, c is the speed of light, and Γ_i is as defined in Sec. III D. In a disk-like parabolic QD with identical confinement strengths ω_l and ω_t for both electrons and holes in the longitudinal and transverse directions, respectively, and based on the assumption that the dot is much smaller than the Bohr radius of the exciton, i.e., $\omega_l, \omega_t \gg V_{\mathrm{Coul}}$ with the Coulomb potential V_{Coul}, the exciton's dipole moment (DM) may be written as $|\mathbf{d}_i| \equiv e|\langle\phi_i(r)|\mathbf{r}|\phi_i(r)\rangle| = el_c$, where $l_c = \sqrt{\hbar/\omega_t\mu^*}$ is the effective cyclotron radius of the exciton and μ^* is its reduced mass.

The optical properties of the ground and first-excited states of a QDM can be demonstrated as follows. Consider a coupled-QD system with bare electron (hole) energies $E_{e1(h1)}$ and $E_{e2(h2)}$ associated with dots 1 and 2, respectively, and with a tunnel strength $t_{e(h)}$ between the dots. The tunneling t and the Coulomb interaction mix the single-QD states of both electron ($|i\rangle_e$, i denotes the dot 1 or 2) and hole ($|i\rangle_h$). In the regime in which confinement and tunnel splitting are predominant over the Coulomb effect, a narrow barrier, the energies of the ground, the excited state of the electron (hole), and their associated wave functions, can be approximated as

$$E_{e(h),g} = 1/2[(E_{e(h)1} + E_{e(h)2}) \mp \sqrt{\Delta E_{e(h)}^2 + 4t_{e(h)}^2}], \tag{6}$$

$$|g\rangle_{e(h)} = \frac{1}{\sqrt{1+\eta_{e(h)}^2}}[\eta_{e(h)}|1\rangle_{e(h)} + |2\rangle_{e(h)}], \tag{7}$$

and

$$E_{e(h),ex} = 1/2[(E_{e(h)1} + E_{e(h)2}) \pm \sqrt{\Delta E_{e(h)}^2 + 4t_{e(h)}^2}], \tag{8}$$

$$|ex\rangle_{e(h)} = \frac{1}{\sqrt{1+\chi_{e(h)}^2}}[\chi_{e(h)}|1\rangle_{e(h)} + |2\rangle_{e(h)}], \tag{9}$$

respectively, where $E_{e(h)1} = \hbar\omega_{le(h)}/2 + \hbar\omega_{te(h)}$, $\eta_{e(h)} = (\Delta E_{e(h)} \pm \sqrt{\Delta E_{e(h)}^2 + 4t_{e(h)}^2})/2t_{e(h)}$, $\chi_{e(h)} = (\Delta E_{e(h)} \mp \sqrt{\Delta E_{e(h)}^2 + 4t_{e(h)}^2})/2t_{e(h)}$, $\Delta E_{e(h)} = E_{e(h)2} - E_{e(h)1}$, and $\omega_{le(h)}$ and $\omega_{te(h)}$ are the confinement strengths of the electron (hole) in the growth and transverse directions. The QDM states of the exciton may have the forms of $|S1\rangle = |g\rangle_e|g\rangle_h$, $|S2\rangle = |g\rangle_e|ex\rangle_h$, $|S3\rangle = |ex\rangle_e|g\rangle_h$, and $|S4\rangle = |ex\rangle_e|ex\rangle_h$. In the double-oscillator approximation and $E_{e(h)1}, E_{e(h)2} \gg \Delta E_{e(h)}$, where $\Delta E_{e(h)}$ is determined mainly by the fluctuation of the dot's height, the tunneling strength of the electron (hole) can be estimated by $t_{e(h)} = \exp(-\alpha_{e(h)}^2)\hbar\omega_{le(h)}\alpha_{e(h)}/\sqrt{\pi}$ with the dimensionless distance $\alpha_{e(h)} = a/l_{e(h)}$ between the oscillator centers at $\pm a$, $l_{e(h)} = \sqrt{\hbar/m_{e(hl)}^*\omega_{le(h)}}$, and $m_{e(hl)}^*$ as the effective mass of an electron (of a hole in the growth direction).[28]

The DMs of these states, including the effect of indirect exciton, can be written as

$$|\mathbf{d}_{S1}| = e\frac{|(1+\eta_e\eta_h)l_c + \sqrt{l_c^2+4a^2}(\eta_e+\eta_h)C\exp[-2a^2/(l_e^2+l_h^2)]|}{\sqrt{1+\eta_e^2}\sqrt{1+\eta_h^2}}, \tag{10}$$

$$|\mathbf{d}_{S2}| = e\frac{|(1+\eta_e\chi_h)l_c + \sqrt{l_c^2+4a^2}(\eta_e+\chi_h)C\exp[-2a^2/(l_e^2+l_h^2)]|}{\sqrt{1+\eta_e^2}\sqrt{1+\chi_h^2}}, \tag{11}$$

$$|\mathbf{d}_{S3}| = e\frac{|(1+\chi_e\eta_h)l_c + \sqrt{l_c^2+4a^2}(\chi_e+\eta_h)C\exp[-2a^2/(l_e^2+l_h^2)]|}{\sqrt{1+\chi_e^2}\sqrt{1+\eta_h^2}}, \tag{12}$$

$$|\mathbf{d}_{S4}| = e\frac{|(1+\chi_e\chi_h)l_c + \sqrt{l_c^2+4a^2}(\chi_e+\chi_h)C\exp[-2a^2/(l_e^2+l_h^2)]|}{\sqrt{1+\chi_e^2}\sqrt{1+\chi_h^2}}, \tag{13}$$

where the effective confined strength ω_t of the exciton can be estimated from $\omega_t = \sqrt{(m_e^*\omega_{te}^2 + m_{ht}^*\omega_{th}^2)/(m_e^* + m_{ht}^*)}$, $C = \sqrt{2l_el_h/(l_e^2+l_h^2)}$, and m_{ht}^* is the effective mass of a hole in the transverse direction. The first term in Eqs. (10)–(13) results from the effect of the intradot (direct) exciton while the second term is associated with the interdot (indirect) exciton. The confinement strengths of an electron (hole) in growth and transverse directions can be approximated by $\omega_{le(h)} = \sqrt{8V_{\mathrm{co(bo)}}/m_{e(hl)}^*h^2}$ and $\omega_{te(h)} = \sqrt{8V_{\mathrm{co(bo)}}/m_{e(ht)}^*R^2}$, respectively, where $V_{\mathrm{co(bo)}}$ is the conduction (valence) band offset, h is the height of the dot, and R is the radius of the dot.

For $m_e^* = 0.081m_0$, $m_{hl}^* = 0.34m_0$, $m_{ht}^* = 0.153m_0$, $V_{\mathrm{co}} = 0.68$ eV, $V_{\mathrm{bo}} = 0.1$ eV, $E_{g(\mathrm{dot})} = 0.73$ eV, $h = 3.5$ nm, $R = 17$ nm, and $\Delta E_h = -\Delta E_e/5$, Figs. 2 and 3 plot the calculated energy levels of the exciton and their DMs in terms of ΔE_e and $2a$ (the distance between the dots), respectively. For a symmetric structure, $\eta_i = 1$ and $\chi_i = -1$, the DMs of the states $|S2\rangle$ and $|S3\rangle$ become zero, representing a dark-exciton state, as presented in Fig. 2(a). ΔE_e increases with the asymmetry and the distribution of the ground state of the electrons and holes tends toward lower energy, while that of the excited state tends toward higher energy. These inhomogeneous dis-

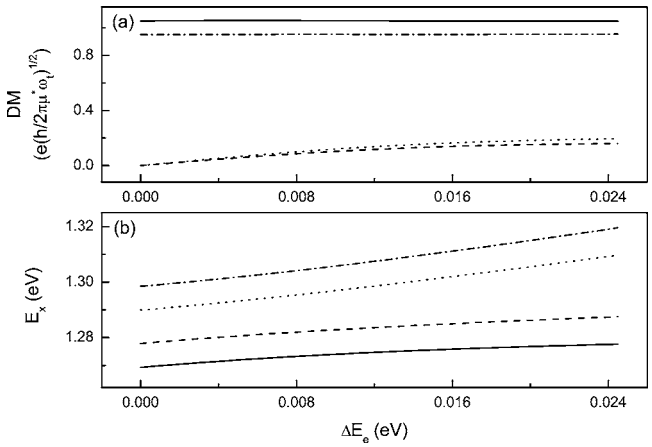

FIG. 2. Calculated (a) DMs and (b) exciton energies in terms of ΔE_e for the states $|S1\rangle$ (solid), $|S2\rangle$ (dash), $|S3\rangle$ (dot), and $|S4\rangle$ (dash-dot) at an interdot distance of 5 nm.

tributions of the electrons and holes increase the DMs of $|S2\rangle$ and $|S3\rangle$. The coupling between the dots declines exponentially with the interdot distance at long distances, as plotted in Fig. 3(c), and the energy differences between $|S1\rangle$ and $|S2\rangle$ and between $|S3\rangle$ and $|S4\rangle$ reasonably reduce to ΔE_h, as plotted in Fig. 3(b). In this situation, the exciton states $|S1\rangle$ and $|S4\rangle$ approach the state of an isolated QD and their DMs reduce to the DMs of the QD; states $|S2\rangle$ and $|S3\rangle$ become a pure indirect exciton and their DMs approach zero, as plotted in Fig. 3(a), because the interdot wave function overlap of the electron and hole approaches zero. At short distances, the tunnel splitting, which exceeds the energy difference caused by the asymmetry of the dots, Fig. 3(c), dominates the DMs of the states $|S2\rangle$ and $|S3\rangle$. Then, the property of the system tends toward that of the symmetric system, and the DMs of the states $|S2\rangle$ and $|S3\rangle$ shrink, as plotted in Fig. 3(a). An increase in the tunneling strength increases the gaps between these four states, as presented in Fig. 3(b). Figure 4 plots the transition rates of these four states with respect to the interdot distance for $\Delta E_e = 15$ meV and $\Delta E_h = 3$ meV. The figure clearly demonstrates that the transition rates of both states $|S2\rangle$ and $|S3\rangle$ are one order smaller than those of states $|S1\rangle$

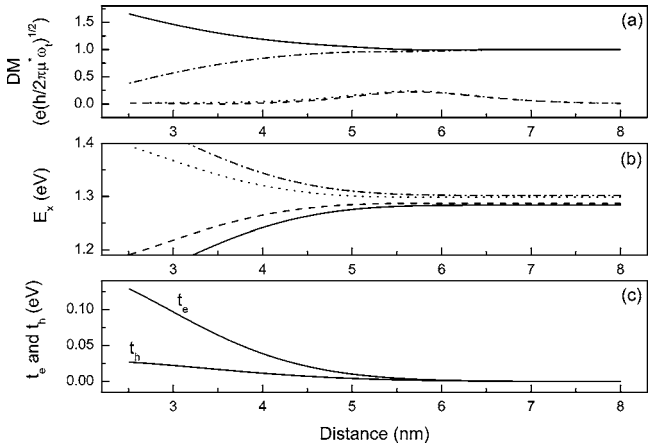

FIG. 3. Calculated (a) DMs, (b) tunneling strengths, and (c) exciton energies with respect to interdot distance in states $|S1\rangle$ (solid), $|S2\rangle$ (dash), $|S3\rangle$ (dot), and $|S4\rangle$ (dash-dot) for $\Delta E_e = 15$ meV.

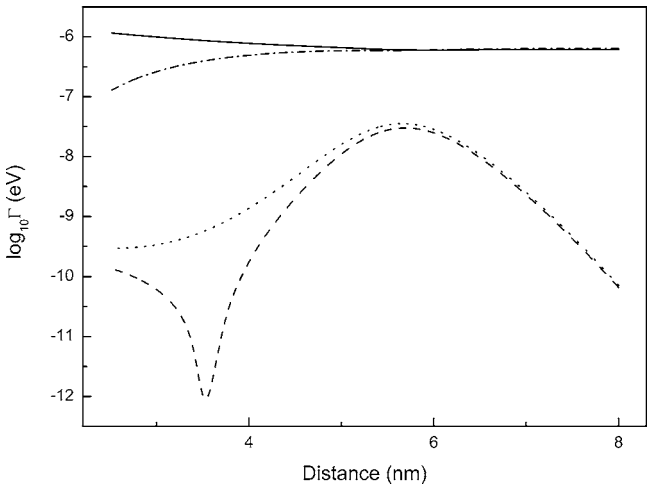

FIG. 4. Calculated transition rates with respect to interdot distance in the states $|S1\rangle$ (solid), $|S2\rangle$ (dash), $|S3\rangle$ (dot), and $|S4\rangle$ (dash-dot) for $\Delta E_e = 15$ meV.

and $|S4\rangle$ over a wide range of distances. Therefore, the lifetime of these states is much longer than that of states of $|S1\rangle$ and $|S4\rangle$. Notably, the transition rate of state $|S1\rangle$ is nearly double that of the single QD (~ 0.61 μeV), which is the value ~ 1.16 μeV at an interdot distance of ~ 2.5 nm because of the contribution of the indirect exciton. The transition rate of QDM (QD) yields an exciton decay time of ~ 0.57 ns (~ 1.1 ns). The calculated results reveal that the model used herein is qualitatively correct.

E. Coupling strengths of LO phonons

In the estimation of LO-phonon coupling strength, LO phonons that are considered to be confined in a cubic quantum box of size ζ with a pressure-free boundary condition. The coupling strength γ_q of mode q has the form[29]

$$\gamma_q = \frac{4e}{|\mathbf{q}|}\sqrt{\frac{\pi\hbar\omega_{\mathrm{LO}}}{\varsigma^3}}\left(\frac{1}{\varepsilon_\infty}-\frac{1}{\varepsilon_0}\right)\sin(q_x x)\sin(q_y y)\sin(q_z z), \tag{14}$$

where ε_∞ and ε_0 are the high frequency and static dielectric constants of the material of the dot. The total coupling strength has been estimated for GaAs QD (Ref. 29) to be

$$\gamma_0 = \sqrt{\sum_q \gamma_q^2} = \frac{0.35\hbar\omega_{\mathrm{LO}}}{\sqrt{\varsigma}}. \tag{15}$$

For InAs QD, the factor 0.35 is simply rescaled by $(\varepsilon_\infty^{-1}-\varepsilon_0^{-1})_{\mathrm{InAs}}/(\varepsilon_\infty^{-1}-\varepsilon_0^{-1})_{\mathrm{GaAs}}$ and takes the value ~ 0.374. For $\zeta \cong 8.56$ nm, which corresponds to the volume of a QD of diameter 20 nm and height 2 nm, and $\hbar\omega_{\mathrm{LO}} = 36$ meV, the total strength is estimated to be ~ 4.6 meV. This result will be used in later discussions.

III. EQUATIONS OF MOTION

A. Approximation

The kinetics of the system can be described by a set of master equations that are obtained by applying the EOM approach

$$i\partial_t\langle\hat{O}\rangle = \langle[\hat{O},\hat{H}]\rangle, \tag{16}$$

to the density operators of exciton, photon, and phonon (in units of $\hbar=1$), and by taking the thermal average over the operator and the commutator. In the derivation of these equations, the following approximations are made:

(1) The small interacting strength between excitons and photons allows the optical transitions to be approximated to the second order, meaning to the orders of $|\gamma_{pg}|^2$ and $|\gamma_{pe}|^2$. In such an approximation, the terms associated with nonconserved photon momentum, such as $\langle\cdots\hat{a}_p^+\hat{a}_{p'}\rangle$, and with multiple-photon processes, such as $\langle\cdots\hat{a}_p^+\hat{a}_{p'}^+\rangle$, are ignored.
(2) The terms with multiple poles, such as $1/[(s-\omega_a)+i\delta][(s-\omega_b)+i\delta]$ in the s plane (a dual space in the Laplace transformation), that are well separated, i.e., $|\omega_a-\omega_b|\gg\delta$ with δ being the broadening width, are neglected.
(3) In the case of low-power excitation, where only one exciton is present in the system, the terms with multiple-exciton processes, such as $\langle\cdots\hat{\alpha}_g\hat{\alpha}_e\rangle$, $\langle\cdots\hat{\alpha}_g^+\hat{n}_{ee}\rangle$, and $\langle\cdots\hat{\alpha}_g^+\hat{\alpha}_g\hat{\alpha}_e\rangle$, are truncated.

Under these approximations, the equation set can be solved analytically.

B. EOMs of density matrix

To describe the time evolution of the densities with multiple varieties, Eq. (16) is first applied to the lowest-order diagonal elements of the densities, yielding the equations

$$i\partial_t\langle\hat{a}_p^+\hat{a}_p\rangle = \gamma_{pi}\langle\hat{a}_p^+\hat{\alpha}_i\rangle - \gamma_{pi}^*\langle\hat{\alpha}_i^+\hat{a}_p\rangle, \tag{17}$$

$$i\partial_t\langle\hat{\alpha}_g^+\hat{\alpha}_g\rangle = -\gamma_{pg}\langle\hat{a}_p^+\hat{\alpha}_g\rangle + \gamma_{pg}^*\langle\hat{\alpha}_g^+\hat{a}_p\rangle + \gamma_1\langle\hat{d}_1^+\hat{\alpha}_g^+\hat{\alpha}_e\rangle - \gamma_1^*\langle\hat{d}_1\hat{\alpha}_e^+\hat{\alpha}_g\rangle, \tag{18}$$

$$i\partial_t\langle\hat{\alpha}_e^+\hat{\alpha}_e\rangle = -\gamma_{pe}\langle\hat{a}_p^+\hat{\alpha}_e\rangle + \gamma_{pe}^*\langle\hat{\alpha}_e^+\hat{a}_p\rangle - \gamma_1\langle\hat{d}_1^+\hat{\alpha}_g^+\hat{\alpha}_e\rangle + \gamma_1^*\langle\hat{d}_1\hat{\alpha}_e^+\hat{\alpha}_g\rangle. \tag{19}$$

The repeated subscripts that do not appear in the left-hand side of the EOMs imply a summation over the subscripts, such as $\gamma_{pi}\langle\hat{a}_p^+\hat{\alpha}_i\rangle=\Sigma_{p,i}\gamma_{pi}\langle\hat{a}_p^+\hat{\alpha}_i\rangle$ and $\gamma_1\langle\hat{d}_1^+\hat{\alpha}_g^+\hat{\alpha}_e\rangle=\Sigma_{q_1}\gamma_{q_1}\langle\hat{d}_{q_1}^+\hat{\alpha}_g^+\hat{\alpha}_e\rangle$. The time evolution of the diagonal densities by the mechanisms of particle transition generates the off-diagonal densities in Eqs. (17)–(19). The dynamics of the off-diagonal densities are determined by applying Eq. (16) again to these newly generated terms, yielding

$$i\partial_t\langle\hat{a}_p^+\hat{\alpha}_g\rangle \cong (E_g-\omega_p)\langle\hat{a}_p^+\hat{\alpha}_g\rangle + \gamma_{pg}^*\langle\hat{a}_p^+\hat{a}_p\rangle - \gamma_{pg}^*\langle\hat{\alpha}_g^+\hat{\alpha}_g\rangle + \gamma_1\langle\hat{d}_1^+\hat{a}_p^+\hat{\alpha}_e\rangle, \tag{20}$$

$$i\partial_t\langle\hat{a}_p^+\hat{\alpha}_e\rangle \cong (E_e-\omega_p)\langle\hat{a}_p^+\hat{\alpha}_e\rangle + \gamma_{pe}^*\langle\hat{a}_p^+\hat{a}_p\rangle - \gamma_{pe}^*\langle\hat{\alpha}_e^+\hat{\alpha}_e\rangle + \gamma_1^*\langle\hat{d}_1\hat{a}_p^+\hat{\alpha}_g\rangle, \tag{21}$$

$$i\partial_t\langle\hat{d}_1^+\hat{\alpha}_g^+\hat{\alpha}_e\rangle \cong (E_e-E_g-\omega_{\mathrm{LO}})\langle\hat{d}_1^+\hat{\alpha}_g^+\hat{\alpha}_e\rangle + \gamma_2^*\langle\hat{d}_1^+\hat{d}_2\hat{\alpha}_g^+\hat{\alpha}_g\rangle - \gamma_2^*\langle\hat{d}_2\hat{d}_1^+\hat{\alpha}_e^+\hat{\alpha}_e\rangle - \gamma_{pg}\langle\hat{d}_1^+\hat{a}_p^+\hat{\alpha}_e\rangle + \gamma_{pe}^*\langle\hat{d}_1^+\hat{\alpha}_g^+\hat{a}_p\rangle, \tag{22}$$

$$i\partial_t\langle\hat{d}_1^+\hat{a}_p^+\hat{\alpha}_e\rangle \cong (E_e-\omega_p-\omega_{\mathrm{LO}})\langle\hat{d}_1^+\hat{a}_p^+\hat{\alpha}_e\rangle + \gamma_{pe}^*\langle\hat{d}_1^+\hat{a}_p^+\hat{a}_p\rangle - \gamma_{pe}^*\langle\hat{d}_1^+\hat{\alpha}_e^+\hat{\alpha}_e\rangle + \gamma_2^*\langle\hat{d}_1^+\hat{d}_2\hat{a}_p^+\hat{\alpha}_g\rangle - \gamma_{pg}^*\langle\hat{d}_1^+\hat{\alpha}_g^+\hat{\alpha}_e\rangle \cong (E_e-\omega_p-\omega_{\mathrm{LO}})\langle\hat{d}_1^+\hat{a}_p^+\hat{\alpha}_e\rangle + \gamma_2^*\langle\hat{d}_1^+\hat{d}_2\hat{a}_p^+\hat{\alpha}_g\rangle - \gamma_{pg}^*\langle\hat{d}_1^+\hat{\alpha}_g^+\hat{\alpha}_e\rangle, \tag{23}$$

where ω_p (ω_{LO}) denotes the photon (LO-phonon) energy and E_i is the energy of the bare exciton in state i. In the derivation, the approximation described in the last section and the identities of Eq. (3) are applied. Notably, the EOMs for the off-diagonal densities have a nonzero pole in the first term of these equations. The terms $\langle d_1^+a_p^+a_p\rangle$ and $\langle d_1^+\alpha_g^+\alpha_g\rangle$ in Eq. (23) can be easily verified to have poles at ω_{LO}, which differs substantially from the pole $E_e-\omega_p-\omega_{\mathrm{LO}}$ for $\langle d_1^+a_p^+\alpha_e\rangle$. They can thus be ignored due to the approximation rule (2).

At first glance, the EOMs seem likely to be endless because the new higher-order terms are generated when Eq. (16) is repeatedly applied to the new terms. Fortunately, recurrence relations apply to the endless EOMs under the approximations that are made herein. They are

$$i\partial_t\langle(\hat{d}_\bullet\hat{d}_\bullet^+)^j\hat{a}_p^+\hat{a}_p\rangle = \gamma_{pi}\langle(\hat{d}_\bullet\hat{d}_\bullet^+)^j\hat{a}_p^+\hat{\alpha}_i\rangle - \gamma_{pi}^*\langle(\hat{d}_\bullet\hat{d}_\bullet^+)^j\hat{\alpha}_i^+\hat{a}_p\rangle, \tag{24}$$

$$i\partial_t\langle(\hat{d}_\bullet^+\hat{d}_\bullet)^j\hat{a}_p^+\hat{a}_p\rangle = \gamma_{pi}\langle(\hat{d}_\bullet^+\hat{d}_\bullet)^j\hat{a}_p^+\hat{\alpha}_i\rangle - \gamma_{pi}^*\langle(\hat{d}_\bullet^+\hat{d}_\bullet)^j\hat{\alpha}_i^+\hat{a}_p\rangle, \tag{25}$$

$$i\partial_t\langle(\hat{d}_\bullet^+\hat{d}_\bullet)^j\hat{\alpha}_g^+\hat{\alpha}_g\rangle = -\gamma_{pg}\langle(\hat{d}_\bullet^+\hat{d}_\bullet)^j\hat{a}_p^+\hat{\alpha}_g\rangle + \gamma_{pg}^*\langle(\hat{d}_\bullet^+\hat{d}_\bullet)^j\hat{\alpha}_g^+\hat{a}_p\rangle + \gamma_{2j+1}\langle(\hat{d}_\bullet^+\hat{d}_\bullet)^j\hat{d}_{2j+1}^+\hat{\alpha}_g^+\hat{\alpha}_e\rangle - \gamma_{2j+1}^*\langle\hat{d}_{2j+1}(\hat{d}_\bullet^+\hat{d}_\bullet)^j\hat{\alpha}_e^+\hat{\alpha}_g\rangle, \tag{26}$$

$$i\partial_t\langle(\hat{d}_\bullet\hat{d}_\bullet^+)^j\hat{\alpha}_e^+\hat{\alpha}_e\rangle = -\gamma_{pe}\langle(\hat{d}_\bullet\hat{d}_\bullet^+)^j\hat{a}_p^+\hat{\alpha}_e\rangle + \gamma_{pe}^*\langle(\hat{d}_\bullet\hat{d}_\bullet^+)^j\hat{\alpha}_e^+\hat{a}_p\rangle - \gamma_{2j+1}\langle\hat{d}_{2j+1}^+(\hat{d}_\bullet\hat{d}_\bullet^+)^j\hat{\alpha}_g^+\hat{\alpha}_e\rangle + \gamma_{2j+1}^*\langle(\hat{d}_\bullet\hat{d}_\bullet^+)^j\hat{d}_{2j+1}\hat{\alpha}_e^+\hat{\alpha}_g\rangle, \tag{27}$$

$$i\partial_t\langle(\hat{d}_\bullet^+\hat{d}_\bullet)^j\hat{d}_{2j+1}^+\hat{\alpha}_g^+\hat{\alpha}_e\rangle = (E_e-E_g-\omega_{\mathrm{LO}})\times\langle(\hat{d}_\bullet^+\hat{d}_\bullet)^j\hat{d}_{2j+1}^+\hat{\alpha}_g^+\hat{\alpha}_e\rangle - \gamma_{pg}\langle(\hat{d}_\bullet^+\hat{d}_\bullet)^j\hat{d}_{2j+1}^+\hat{a}_p^+\hat{\alpha}_e\rangle + \gamma_{pe}^*\langle(\hat{d}_\bullet^+\hat{d}_\bullet)^j\hat{d}_{2j+1}^+\hat{\alpha}_g^+\hat{a}_p\rangle + \gamma_{2j+2}^*\langle(\hat{d}_\bullet^+\hat{d}_\bullet)^{j+1}\hat{\alpha}_g^+\hat{\alpha}_g\rangle - \gamma_{2j+2}^*\langle(\hat{d}_\bullet\hat{d}_\bullet^+)^{j+1}\hat{\alpha}_e^+\hat{\alpha}_e\rangle, \tag{28}$$

$$i\partial_t\langle(\hat{d}_\bullet^+\hat{d}_\bullet)^j\hat{a}_p^+\hat{\alpha}_g\rangle = (E_g-\omega_p)\langle(\hat{d}_\bullet^+\hat{d}_\bullet)^j\hat{a}_p^+\hat{\alpha}_g\rangle + \gamma_{pg}^*\langle(\hat{d}_\bullet^+\hat{d}_\bullet)^j\hat{a}_p^+\hat{a}_p\rangle - \gamma_{pg}^*\langle(\hat{d}_\bullet^+\hat{d}_\bullet)^j\hat{\alpha}_g^+\hat{\alpha}_g\rangle + \gamma_{2j+1}\langle(\hat{d}_\bullet^+\hat{d}_\bullet)^j\hat{d}_{2j+1}^+\hat{a}_p^+\hat{\alpha}_e\rangle, \quad (29)$$

$$i\partial_t\langle(\hat{d}_\bullet\hat{d}_\bullet^+)^j\hat{a}_p^+\hat{\alpha}_e\rangle = (E_e-\omega_p)\langle(\hat{d}_\bullet\hat{d}_\bullet^+)^j\hat{a}_p^+\hat{\alpha}_e\rangle + \gamma_{pe}^*\langle(\hat{d}_\bullet\hat{d}_\bullet^+)^j\hat{a}_p^+\hat{a}_p\rangle - \gamma_{pe}^*\langle(\hat{d}_\bullet\hat{d}_\bullet^+)^j\hat{\alpha}_e^+\hat{\alpha}_e\rangle + \gamma_{2j+1}^*\langle(\hat{d}_\bullet\hat{d}_\bullet^+)^j\hat{d}_{2j+1}\hat{a}_p^+\hat{\alpha}_g\rangle, \quad (30)$$

$$i\partial_t\langle(\hat{d}_\bullet^+\hat{d}_\bullet)^j\hat{d}_{2j+1}^+\hat{a}_p^+\hat{\alpha}_e\rangle = (E_e-\omega_p-\omega_{\mathrm{LO}})\langle(\hat{d}_\bullet^+\hat{d}_\bullet)^j\hat{d}_{2j+1}^+\hat{a}_p^+\hat{\alpha}_e\rangle + \gamma_{2j+2}^*\langle(\hat{d}_\bullet^+\hat{d}_\bullet)^{j+1}\hat{a}_p^+\hat{\alpha}_g\rangle - \gamma_{pg}^*\langle(\hat{d}_\bullet^+\hat{d}_\bullet)^j\hat{d}_{2j+1}^+\hat{\alpha}_g^+\hat{\alpha}_e\rangle, \quad (31)$$

$$i\partial_t\langle(\hat{d}_\bullet^+\hat{d}_\bullet)^j\hat{d}_{2j+1}^+\hat{\alpha}_g^+\hat{a}_p\rangle = (\omega_p-E_g-\omega_{\mathrm{LO}})\times\langle(\hat{d}_\bullet^+\hat{d}_\bullet)^j\hat{d}_{2j+1}^+\hat{\alpha}_g^+\hat{a}_p\rangle - \gamma_{2j+2}^*\langle(\hat{d}_\bullet\hat{d}_\bullet^+)^{j+1}\hat{\alpha}_e^+\hat{a}_p\rangle + \gamma_{pe}\langle(\hat{d}_\bullet^+\hat{d}_\bullet)^j\hat{d}_{2j+1}^+\hat{\alpha}_g^+\hat{\alpha}_e\rangle, \quad (32)$$

with $(\hat{d}_\bullet^+\hat{d}_\bullet)^j=\hat{d}_1^+\hat{d}_2\cdots\hat{d}_{2j-1}^+\hat{d}_{2j}$. For $j=0$, Eqs. (24)–(27) become Eqs. (17)–(19). Solving these equations with a proper initial condition yields the time evolution of the population densities.

C. Initial conditions

The initial conditions on the densities govern the solutions to Eqs. (24)–(32). In the sudden approximation, the Hamiltonian changes abruptly because of the sudden change in the populations at $t=0$ and the wave function is therefore expected not to change much at the initial time and the system is expected to remain in approximate equilibrium. In this situation, the thermal average of the off-diagonal densities approaches zero,[30] while the diagonal densities have the form, for example,

$$\langle(\hat{d}_\bullet^+\hat{d}_\bullet)^j\hat{\alpha}_i^+\hat{\alpha}_i\rangle_0 = \delta_{\bullet,\bullet}\langle(\hat{d}_\bullet^+\hat{d}_\bullet)^j\rangle_0 N_i(0). \quad (33)$$

The delta function with the subscript • means that the phonon operators have to be paired in all possible combinations, such as for the term with four phonon operators[30]

$$\delta_{\bullet,\bullet}\langle\hat{d}_1^+\hat{d}_2\hat{d}_3^+\hat{d}_4\rangle_0 = (\delta_{1,2}\delta_{3,4}+\delta_{1,4}\delta_{2,3})\langle\hat{d}_1^+\hat{d}_2\hat{d}_3^+\hat{d}_4\rangle_0 = \delta_{1,2}\delta_{3,4}N_B^2+\delta_{1,4}\delta_{2,3}N_B(1+N_B) \quad (34)$$

with Planck's distribution N_B and the initial number of photons (excitons) $N_p(0)\equiv\langle\hat{a}_p^+\hat{a}_p\rangle_0$ $[N_i(0)\equiv\langle\hat{\alpha}_i^+\hat{\alpha}_i\rangle_0]$. The first term in Eq. (34) results from the direct LO-phonon process, while the second results from the exchange LO-phonon process.

D. EOMs in *S* plane

Solving the differential Eqs. (24)–(32) is facilitating by transforming them into an algebraic problem by applying the Laplace transformation, defined as $\bar{N}(s)=\int_0^\infty N(t)\exp(-st)dt$, with the initial conditions that were stated in the preceding section. Laplace transforms of the equations yield

$$is\overline{\langle(\hat{d}_\bullet\hat{d}_\bullet^+)^j\hat{a}_p^+a_p\rangle} = i\delta_{\bullet,\bullet}\langle(\hat{d}_\bullet\hat{d}_\bullet^+)^j\hat{a}_p^+\hat{a}_p\rangle_0 + \gamma_{pe}\overline{\langle(\hat{d}_\bullet\hat{d}_\bullet^+)^j\hat{a}_p^+\hat{\alpha}_e\rangle} - \gamma_{pe}^*\overline{\langle(\hat{d}_\bullet\hat{d}_\bullet^+)^j\hat{\alpha}_e^+\hat{a}_p\rangle}, \quad (24')$$

$$is\overline{\langle(\hat{d}_\bullet^+\hat{d}_\bullet)^j\hat{a}_p^+\hat{a}_p\rangle} = i\delta_{\bullet,\bullet}\langle(\hat{d}_\bullet^+\hat{d}_\bullet)^j\hat{a}_p^+\hat{a}_p\rangle_0 + \gamma_{pg}\overline{\langle(\hat{d}_\bullet^+\hat{d}_\bullet)^j\hat{a}_p^+\hat{\alpha}_g\rangle} - \gamma_{pg}^*\overline{\langle(\hat{d}_\bullet^+\hat{d}_\bullet)^j\hat{\alpha}_g^+\hat{a}_p\rangle}, \quad (25')$$

$$is\overline{\langle(\hat{d}_\bullet^+\hat{d}_\bullet)^j\hat{\alpha}_g^+\hat{\alpha}_g\rangle} = i\delta_{\bullet,\bullet}\langle(\hat{d}_\bullet^+\hat{d}_\bullet)^j\hat{\alpha}_g^+\hat{\alpha}_g\rangle_0 - \gamma_{pg}\overline{\langle(\hat{d}_\bullet^+\hat{d}_\bullet)^j\hat{a}_p^+\hat{\alpha}_g\rangle} + \gamma_{pg}^*\overline{\langle(\hat{d}_\bullet^+\hat{d}_\bullet)^j\hat{\alpha}_g^+\hat{a}_p\rangle} + \gamma_{2j+1}\overline{\langle(\hat{d}_\bullet^+\hat{d}_\bullet)^j\hat{d}_{2j+1}^+\hat{\alpha}_g^+\hat{\alpha}_e\rangle} - \gamma_{2j+1}^*\overline{\langle\hat{d}_{2j+1}(\hat{d}_\bullet^+\hat{d}_\bullet)^j\hat{\alpha}_e^+\hat{\alpha}_g\rangle}, \quad (26')$$

$$is\overline{\langle(\hat{d}_\bullet\hat{d}_\bullet^+)^j\hat{\alpha}_e^+\hat{\alpha}_e\rangle} = i\delta_{\bullet,\bullet}\langle(\hat{d}_\bullet\hat{d}_\bullet^+)^j\hat{\alpha}_e^+\hat{\alpha}_e\rangle_0 - \gamma_{pe}\overline{\langle(\hat{d}_\bullet\hat{d}_\bullet^+)^j\hat{a}_p^+\hat{\alpha}_e\rangle} + \gamma_{pe}^*\overline{\langle(\hat{d}_\bullet\hat{d}_\bullet^+)^j\hat{\alpha}_e^+\hat{a}_p\rangle} - \gamma_{2j+1}\overline{\langle\hat{d}_{2j+1}^+(\hat{d}_\bullet\hat{d}_\bullet^+)^j\hat{\alpha}_g^+\hat{\alpha}_e\rangle} + \gamma_{2j+1}^*\overline{\langle(\hat{d}_\bullet\hat{d}_\bullet^+)^j\hat{d}_{2j+1}\hat{\alpha}_e^+\hat{\alpha}_g\rangle}, \quad (27')$$

$$is\overline{\langle(\hat{d}_\bullet^+\hat{d}_\bullet)^j\hat{d}_{2j+1}^+\hat{\alpha}_g^+\hat{\alpha}_e\rangle} = (E_e-E_g-\omega_{\mathrm{LO}})\overline{\langle(\hat{d}_\bullet^+\hat{d}_\bullet)^j\hat{d}_{2j+1}^+\hat{\alpha}_g^+\hat{\alpha}_e\rangle} - \gamma_{pg}\overline{\langle(\hat{d}_\bullet^+\hat{d}_\bullet)^j\hat{d}_{2j+1}^+\hat{a}_p^+\hat{\alpha}_e\rangle} + \gamma_{pe}^*\overline{\langle(\hat{d}_\bullet^+\hat{d}_\bullet)^j\hat{d}_{2j+1}^+\hat{\alpha}_g^+\hat{a}_p\rangle} + \gamma_{2j+2}^*\overline{\langle(\hat{d}_\bullet^+\hat{d}_\bullet)^{j+1}\hat{\alpha}_g^+\hat{\alpha}_g\rangle} - \gamma_{2j+2}^*\overline{\langle(\hat{d}_\bullet\hat{d}_\bullet^+)^{j+1}\hat{\alpha}_e^+\hat{\alpha}_e\rangle}, \quad (28')$$

$$is\overline{\langle(\hat{d}_\bullet^+\hat{d}_\bullet)^j\hat{a}_p^+\hat{\alpha}_g\rangle} = (E_g-\omega_p)\overline{\langle(\hat{d}_\bullet^+\hat{d}_\bullet)^j\hat{a}_p^+\hat{\alpha}_g\rangle} + \gamma_{pg}^*\overline{\langle(\hat{d}_\bullet^+\hat{d}_\bullet)^j\hat{a}_p^+\hat{a}_p\rangle} - \gamma_{pg}^*\overline{\langle(\hat{d}_\bullet^+\hat{d}_\bullet)^j\hat{\alpha}_g^+\hat{\alpha}_g\rangle} + \gamma_{2j+1}\overline{\langle(\hat{d}_\bullet^+\hat{d}_\bullet)^j\hat{d}_{2j+1}^+\hat{a}_p^+\hat{\alpha}_e\rangle}, \quad (29')$$

$$is\overline{\langle(\hat{d}_\bullet\hat{d}_\bullet^+)^j\hat{a}_p^+\hat{\alpha}_e\rangle} = (E_e-\omega_p)\overline{\langle(\hat{d}_\bullet\hat{d}_\bullet^+)^j\hat{a}_p^+\hat{\alpha}_e\rangle} + \gamma_{pe}^*\overline{\langle(\hat{d}_\bullet\hat{d}_\bullet^+)^j\hat{a}_p^+\hat{a}_p\rangle} - \gamma_{pe}^*\overline{\langle(\hat{d}_\bullet\hat{d}_\bullet^+)^j\hat{\alpha}_e^+\hat{\alpha}_e\rangle} + \gamma_{2j+1}^*\overline{\langle(\hat{d}_\bullet\hat{d}_\bullet^+)^j\hat{d}_{2j+1}\hat{a}_p^+\hat{\alpha}_g\rangle}, \quad (30')$$

$$is\overline{\langle(\hat{d}_\bullet^+\hat{d}_\bullet)^j\hat{d}_{2j+1}^+\hat{a}_p^+\hat{\alpha}_e\rangle} = (E_e-\omega_p-\omega_{\mathrm{LO}})\overline{\langle(\hat{d}_\bullet^+\hat{d}_\bullet)^j\hat{d}_{2j+1}^+\hat{a}_p^+\hat{\alpha}_e\rangle} + \gamma_{2j+2}^*\overline{\langle(\hat{d}_\bullet^+\hat{d}_\bullet)^{j+1}\hat{a}_p^+\hat{\alpha}_g\rangle} - \gamma_{pg}^*\overline{\langle(\hat{d}_\bullet^+\hat{d}_\bullet)^j\hat{d}_{2j+1}^+\hat{\alpha}_g^+\hat{\alpha}_e\rangle}, \quad (31')$$

$$is\overline{\langle(\hat{d}_\bullet^+\hat{d}_\bullet)^j\hat{d}_{2j+1}^+\hat{\alpha}_g^+\hat{a}_p\rangle} = (\omega_p - E_g - \omega_{\mathrm{LO}})\overline{\langle(\hat{d}_\bullet^+\hat{d}_\bullet)^j\hat{d}_{2j+1}^+\hat{\alpha}_g^+\hat{a}_p\rangle} - \gamma_{2j+2}^*\overline{\langle(\hat{d}_\bullet\hat{d}_\bullet^+)^{j+1}\hat{\alpha}_e^+\hat{a}_p\rangle} + \gamma_{pe}\overline{\langle(\hat{d}_\bullet^+\hat{d}_\bullet)^j\hat{d}_{2j+1}^+\hat{\alpha}_g^+\hat{\alpha}_e\rangle}. \quad (32')$$

Algebraically solving these equations yields the density matrix in the s domain.

In indirect excitation, the initial number of photons with the energies around the ground and excited states of the exciton is zero, i.e., $N_p(0)=0$. This condition yields the solutions to Eqs. (26′) and (27′) with the recurrence relations between the orders j and $j+1$,

$$\overline{\langle(\hat{d}_\bullet^+\hat{d}_\bullet)^j\hat{\alpha}_g^+\hat{\alpha}_g\rangle} = \frac{\delta_{\bullet,\bullet}\langle(\hat{d}_\bullet^+\hat{d}_\bullet)^j\rangle_0 N_g(0)}{(s+2\Gamma_g)} - \frac{2\gamma_{2j+1}^*\gamma_{2j+2}(s+\Gamma_g+\Gamma_e)[\overline{\langle(\hat{d}_\bullet^+\hat{d}_\bullet)^{j+1}\hat{\alpha}_g^+\hat{\alpha}_g\rangle} - \overline{\langle(\hat{d}_\bullet\hat{d}_\bullet^+)^{j+1}\hat{\alpha}_e^+\hat{\alpha}_e\rangle}]}{(s+2\Gamma_g)[(s+\Gamma_g+\Gamma_e)^2+(E_e-E_g-\omega_{\mathrm{LO}}-E_{Ng}+E_{Ne})^2]}, \quad (35)$$

$$\overline{\langle(\hat{d}_\bullet\hat{d}_\bullet^+)^j\hat{\alpha}_e^+\hat{\alpha}_e\rangle} = \frac{\delta_{\bullet,\bullet}\langle(\hat{d}_\bullet\hat{d}_\bullet^+)^j\rangle_0 N_e(0)}{(s+2\Gamma_e)} + \frac{2\gamma_{2j+1}^*\gamma_{2j+2}(s+\Gamma_g+\Gamma_e)[\overline{\langle(\hat{d}_\bullet^+\hat{d}_\bullet)^{j+1}\hat{\alpha}_g^+\hat{\alpha}_g\rangle} - \overline{\langle(\hat{d}_\bullet\hat{d}_\bullet^+)^{j+1}\hat{\alpha}_e^+\hat{\alpha}_e\rangle}]}{(s+2\Gamma_e)[(s+\Gamma_g+\Gamma_e)^2+(E_e-E_g-\omega_{\mathrm{LO}}-E_{Ng}+E_{Ne})^2]}, \quad (36)$$

where the optical-transition rate is defined as $\Gamma_{g(e)} \equiv \mathrm{Re}\{\Sigma_p\gamma_{pg(e)}^2/[s-i(E_{g(e)}-\omega_p)]\}$ and the renormalization energy that is produced by the excitonic polaron coupling to the photons is given by $E_{Ng(e)}=\mathrm{Im}\{\Sigma_p\gamma_{pg(e)}^2/[s-i(E_{e(g)}-\omega_p-\omega_{\mathrm{LO}})]\}$.

E. Analytical solutions

Equations (35) and (36) can be solved step by step, starting from the lowest-order equations, $j=0$. The equations for each order are terminated at the first (initial) term that is governed by the initial conditions for that order, and the other terms will be related to its higher-order ones. Many combinations for the initial term of $j>1$ exist as described in Sec. III C. The choice of combinations depends on the initial term in the last order. For example, one combination $\delta_{1,2}$ ($\delta_{1,2}\langle\hat{d}_1^+\hat{d}_2\rangle_0$) of the initial term exists only to the first order; two combinations $\delta_{1,2}\delta_{3,4}$ and $\delta_{1,4}\delta_{2,3}$ exist to the second order—and so on to the higher orders. If the contribution from the initial term of $j=1$ is considered, then the exchange term ($\delta_{1,4}\delta_{2,3}$) of $j=2$ disappears. By analogy, only one combination exists, and is

$$\delta_{\bullet,\bullet}\langle(\hat{d}_\bullet^+\hat{d}_\bullet)^j\rangle_0 = \delta_{1,2}\delta_{3,4}\cdots\delta_{2j-1,2j}\langle\hat{d}_1^+\hat{d}_2\hat{d}_3^+\hat{d}_4\cdots\hat{d}_{2j-1}^+\hat{d}_{2j}\rangle_0 = \delta_{1,2}\delta_{3,4}\cdots\delta_{2j-1,2j}N_B^j,$$

in counting the contribution from every order that is smaller than j. Since the exciton interacts with the LO phonon such that the exciton emits and then absorbs the same phonon coherently, this phonon is called a resonant phonon.

Iterative substitution of Eqs. (35) and (36) for the order $j+1$ into the equations for order j yields

$$\bar{N}_g(s) = \overline{\langle\hat{\alpha}_g^+\hat{\alpha}_g\rangle} = P_gN_g(0) - 2P_g^2Q\delta_{1,2}\gamma_1^*\gamma_2[\langle\hat{d}_1^+\hat{d}_2\rangle_0N_g(0) - \langle\hat{d}_1\hat{d}_2^+\rangle_0N_e(0)] + 4P_g^3Q^2\delta_{1,2}\delta_{3,4}\gamma_1^*\gamma_2\gamma_3^*\gamma_4[\langle\hat{d}_1^+\hat{d}_2\hat{d}_3^+\hat{d}_4\rangle_0N_g(0) - \langle\hat{d}_1\hat{d}_2^+\hat{d}_3\hat{d}_4^+\rangle_0N_e(0)] - + \cdots \quad (37)$$

and

$$\bar{N}_e(s) = \overline{\langle\hat{\alpha}_e^+\hat{\alpha}_e\rangle} = P_eN_e(0) + 2P_e^2Q\delta_{1,2}\gamma_1^*\gamma_2[\langle\hat{d}_1^+\hat{d}_2\rangle_0N_g(0) - \langle\hat{d}_1\hat{d}_2^+\rangle_0N_e(0)] + 4P_e^3Q^2\delta_{1,2}\delta_{3,4}\gamma_1^*\gamma_2\gamma_3^*\gamma_4[\langle\hat{d}_1^+\hat{d}_2\hat{d}_3^+\hat{d}_4\rangle_0N_g(0) - \langle\hat{d}_1\hat{d}_2^+\hat{d}_3\hat{d}_4^+\rangle_0N_e(0)] - + \cdots, \quad (38)$$

where $P_i \equiv 1/(s+2\Gamma_i)$ and $Q \equiv (s+\Gamma_g+\Gamma_e)/[(s+\Gamma_g+\Gamma_e)^2+\Delta^2]$ with the detuning energy $\Delta \equiv E_e-E_g-\omega_{\mathrm{LO}}-E_{Ng}+E_{Ne}$.

Applying the aforementioned initial conditions and the identity $1/(1+x)=1-x+x^2-+\cdots$ to Eqs. (37) and (38) yields $\bar{N}_g(s)$ and $\bar{N}_e(s)$ in Dyson's form

$$\bar{N}_g(s) = N_g(0)\frac{P_g(1+\gamma_0^2P_eQN_B)}{1+(P_g+P_e)\gamma_0^2QN_B} + N_e(0)\frac{P_gP_e\gamma_0^2Q(1+N_B)}{1+(P_g+P)_e\gamma_0^2Q(1+N_B)} \quad (39)$$

and

$$\bar{N}_e(s) = N_e(0)\frac{P_e[1+\gamma_0^2P_gQ(1+N_B)]}{1+(P_g+P_e)\gamma_0^2Q(1+N_B)} + N_g(0)\frac{P_gP_e\gamma_0^2QN_B}{1+(P_g+P_e)\gamma_0^2QN_B}, \quad (40)$$

with the total strength $\gamma_0=(\Sigma_q|\gamma_q|^2)^{1/2}$ of the interaction of the exciton with all LO-phonon modes. The term $s+\Gamma_e+\Gamma_g$ in the denominator of Q usually is negligible, and keeping this term results in RO, because its value (of the order of micro-electron-volts) is typically much smaller than Δ (of the order of milli-electron-volts) for InGaAs/GaAs QDs and QDMs. Such an approximation, which is equivalent to removing the RO by filtering out the high-frequency signal in the responses of time-resolved PL (TRPL), yields $\gamma_0^2Q \cong 2(s+\Gamma_e+\Gamma_g)\beta^2$ with the dimensionless strength $\beta \equiv \gamma_0/\Delta$. Notably, the square of β times the phonon distribution N_B is the number of LO phonons that clothe an exciton.[31]

For $T=0$, Eqs. (39) and (40) reduce to

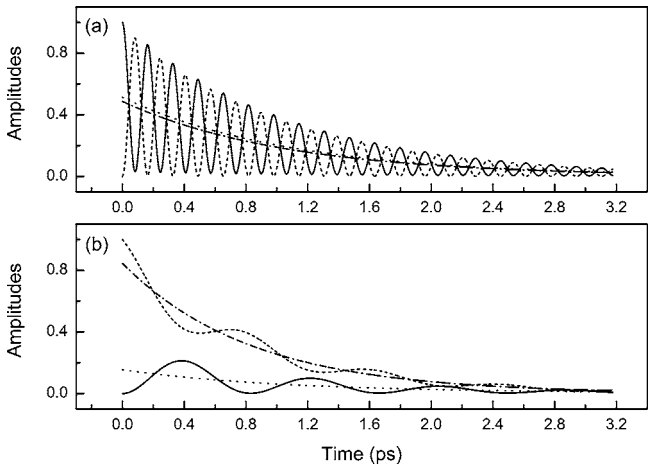

FIG. 5. Time evolution of the excitonic densities in the ground state (dash) and the excited state (solid) with the parameters of $\omega_{\mathrm{LO}}=36$ meV, $\Gamma_g=0.1$ meV, $\Gamma_e=0.5\Gamma_g$, $\gamma_0=3$ meV, $\Delta=1$ meV, and the initial conditions of (a) $N_g(0)=0$ and $N_e(0)=1$ and (b) $N_g(0)=1$ and $N_e(0)=0$ at $T=95$ K. The calculated angular frequencies for the conditions of (a) and (b) are, respectively, ~ 6.12 meV/$\hbar$ and ~ 1.2 meV/$\hbar$. The dot (dash-dot) line displays the density of $N_e(t)$ $[N_g(t)]$ with RO removed for $\beta=3$.

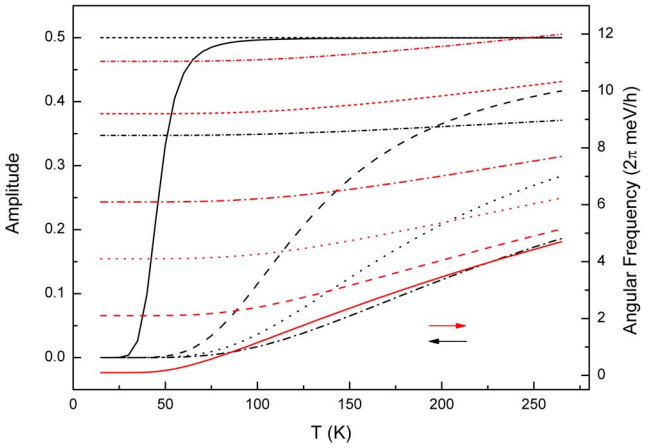

FIG. 6. (Color online) Oscillating frequency (gray) and oscillating amplitude (black) of the RO with the parameters of $\Gamma_g=0.355$ μeV, $\Gamma_e=0$, $\gamma_0=4.6$ meV for $\Delta=0.1$ meV (solid), 2.1 meV (dash), 4.1 meV (dot), and 6.1 meV (dash-dot) with the initial conditions of $N_g(0)=1$ and $N_e(0)=0$ and for $\Delta=0.1$ meV (short dash) and 6.1 meV (short dash-dot) with the conditions of $N_g(0)=0$ and $N_e(0)=1$.

$$\bar{N}_g(s)=N_g(0)P_g+N_e(0)\frac{P_gP_e\gamma_0^2Q}{1+(P_g+P_e)\gamma_0^2Q} \tag{41}$$

and

$$\bar{N}_e(s)=N_e(0)\frac{P_e[1+\gamma_0^2P_gQ]}{1+(P_g+P_e)\gamma_0^2Q}, \tag{42}$$

where the spontaneous emission gives a nonzero dependence on $N_e(0)$ for both $\bar{N}_g(s)$ and $\bar{N}_e(s)$. For $N_g(0)=1$ and $N_e(0)=0$, the decay rate is $2\Gamma_g$ and the RO disappears. For $N_g(0)=0$ and $N_e(0)=1$, the decay rate approximates $\Gamma_g+\Gamma_e$ as $\beta\to\infty$, which can be easily checked by removing RO, and the RO occurs for $\gamma_0>0$. Since the optical transition rates are much smaller than the phonon transition rate, the angular frequency of RO for $T\neq 0$ has the simple form that is obtained by setting $\Gamma_g=\Gamma_e=0$,

$$\omega_{\mathrm{RO}}=\sqrt{\Delta^2+4N_B\gamma_0^2} \tag{43}$$

for $N_g(0)=1$ and $N_e(0)=0$ and

$$\omega_{\mathrm{RO}}=\sqrt{\Delta^2+4(1+N_B)\gamma_0^2} \tag{44}$$

for $N_g(0)=0$ and $N_e(0)=1$. The oscillating frequency of RO in the latter case is less sensitive to T than it is in the former case.

IV. NUMERICAL RESULTS AND DISCUSSIONS

The TRPL intensity of the line feature of state $|i\rangle$ can be related to the excitonic density $N_i(t)$ by $S(t)\propto|N_i(t)|^2$. Inverse Laplace transforms of Eqs. (39) and (40) yield the time evolutions of $N_g(t)$ and $N_e(t)$, respectively. The extreme dissimilarity between the decay time and the oscillating period of RO makes displaying both the time decay and the period in one figure difficult. An unusual transition rate $\Gamma_g=0.1$ meV of the state $|g\rangle$ is used in the calculation of Fig. 5 to demonstrate these features without loss of generality. In the figure, the ROs appear coherently with a phase separation π between N_g and N_e, because the exciton that is coherently mediated by the LO phonons moves up and down between these states. The periods of oscillations for both $N_g(0)=0$ and $N_e(0)=1$ [Fig. 5(a)] and $N_g(0)=1$ and $N_e(0)=0$ [Fig. 5(b)] are consistent with the results calculated from Eqs. (43) and (44). Their values are estimated to be ~ 0.16 and ~ 0.83 ps, respectively. The increase in temperature increases the transition probability and thus increases the amplitude and frequency of oscillation. The figure also reveals the numerical results for $N_e(t)$ (dot) and $N_g(t)$ (dash-dot) when the RO is removed. These results well describe the time decay of the excitonic densities and are used to extract the decay time by simple-exponential fitting.

The amplitude and frequency of the RO depend remarkably on the initial distribution of the excitonic population. For $N_g(0)=1$ and $N_e(0)=0$, the resonant-round trip of the exciton between $|g\rangle$ and $|e\rangle$ is stimulated and continued by repeatedly absorbing and emitting a LO phonon with the momentum q of the phonon. In this case, the amplitude and frequency are very sensitive to T and Δ (see Fig. 6); both increase with T, because an increase in the number of phonons around the exciton increases the probability of phonon-assisted transition. In the calculation of Fig. 6, the parameters of $\gamma_0=4.6$ meV and $\Gamma_g\cong 0.355$ μeV (for a wide range ~ 10 meV of detuning energy), estimated in Sec. II with an interdot distance ~ 4.2 nm, are used. At high T, an identical occupation probability in both states causes the amplitude to approach its maximum 0.5 because of particle conservation $N_g(0)+N_e(0)=1$ for only one exciton in the system. For $N_g(0)=0$ and $N_e(0)=1$, the exciton that is initially in the excited state moves down and up between the states by spontaneously emitting a LO phonon and, then, absorbing this phonon. The spontaneous emission of the LO phonon causes the resonant-round trips even at $T=0$. In this case, the amplitude and frequency are insensitive to T and Δ.

Simple-exponential fitting is used to extract the decay time from the curves calculated from Eqs. (39) and (40) with RO removed, to determine the decay times for these systems.

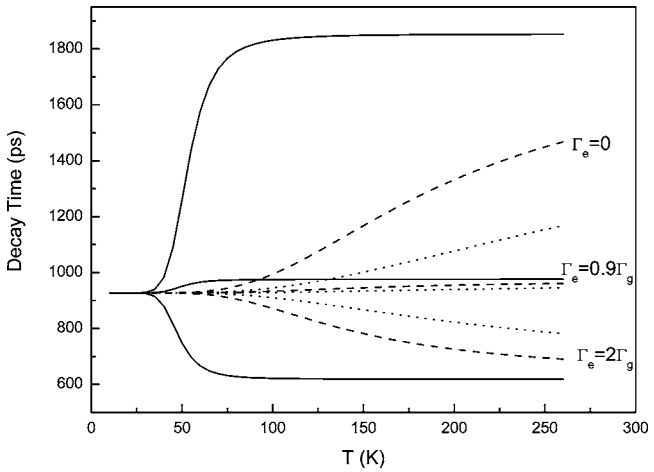

FIG. 7. Decay time as a function of T and Γ_e for β=1.12 (dash), β=2.19 (dot), and β=46 (solid) with the initial conditions of $N_g(0)=1$ and $N_e(0)=0$.

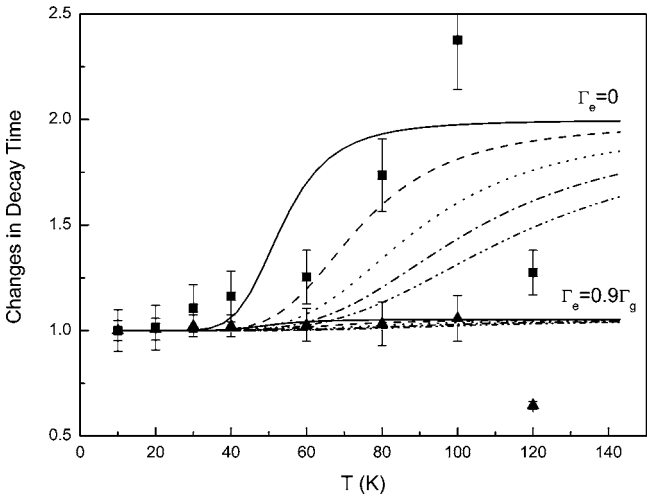

FIG. 8. Changes in decay time relative to that of T=0 as a function of T and Γ_e for β=5.11 (dash-dot-dot), β=6.57 (dash-dot), β=9.2 (dot), β=15.3 (dash), and β=46 (solid), with the initial conditions of $N_g(0)=1$ and $N_e(0)=0$. The solid square (triangle) denotes the experimental results of InGaAs QDMs (Ref. 6) (InGaAs QDs) (Ref. 6).

In the limit β=0 and/or T=0 with the exciton initially in the state $|g\rangle$, zero phonon decouples these states, and the decay rate of the exciton is solely determined by the spontaneous-emission (SE) rate Γ_g of the state $|g\rangle$. At finite T and $\beta \neq 0$, the exciton distribution dominates the decay rate, which takes the form $N_{gNRO}(0^+)\Gamma_g + N_{eNRO}(0^+)\Gamma_e$. In the limit $\beta \rightarrow \infty$ and/or $T \rightarrow \infty$, the exciton has a probability $\sim$0.5 of staying either state $|g\rangle$ and $|e\rangle$ with the decay rate $(\Gamma_g + \Gamma_e)/2$. The decay rate is one half of the SE rate (or double its corresponding decay time) for a fully dark state Γ_e=0 and slightly changes for Γ_e=0.9Γ_g. In an excited state that is brighter than the ground state, such as $2\Gamma_g$, the decay rate increases to three halves of the SE rate. Figure 7 presents all of these features. Since the brightness of the excited state of a QDM system vanishes for a symmetric structure or is weak for an asymmetric structure, the maximal increase in its decay time at high T approaches 2. This result is comparable with the experimental value, which slightly exceeds 2 (solid square in Fig. 8). This result is different from that for QD systems, in which the brightness of the excited state is similar to that of the ground state. Therefore, a change in the decay time (solid triangle) with T is not conspicuous. The experimental data also show a rapid decease in decay time as $T > 100$ K for both QD and QDM, because of thermal emission of the carriers from the QD/QDM, which is neglected in this investigation.

V. CONCLUSION

The theory of exciton coupling to photons and LO phonons in QDs/QDMs was derived. Resonant-round trips of excitons between the ground and excited states, mediated by LO phonons, alter the decay time and produce a RO. The decay time depends strongly on the brightness of the excited state: a dark state enhances the decay time (as for QDMs), and a bright state reduces the decay time (as for QDs). It also depends strongly on the detuning energy between the states. A three-level system that is mediated by a one-phonon process maximally enhances the decay time by a factor of 2. In the strong coupling regime, multiple levels with multiple-phonon processes must be considered, since the manifold loops of polaron resonance that are mediated by multiple phonons can also affect the decay time. For example, two forms of polaron resonance involve a two-phonon process, as schematically plotted in Fig. 9. In the first [Fig. 9(a)], the exciton takes more time than in the three-level system to make a resonant-round trip between the states $|g\rangle$, $|e1\rangle$ and $|e2\rangle$. At high T and/or in the strong coupling region, the identical probabilities $(\sim 1/3)$ that the exciton is in these states reduces the decay rate to one-third that at zero-T. The second [Fig. 9(b)] form of resonance reduces the decay rate to not less than that in the three-level system, because the exciton has a probability of $\sim 1/2$ of remaining in state $|g\rangle$ and a probability of $\sim 1/4$ of being in each of the states $|e1\rangle$ and $|e2\rangle$. In conclusion, the increase in the excitonic decay time in QDs/QDMs is caused by the overall effect of multiple weak-bright excited states or that of a major state with weak-optical transition and a small detuning energy. More-

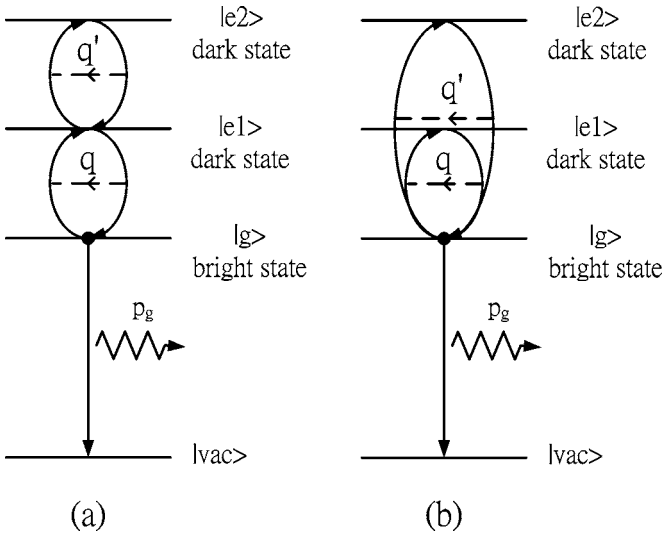

FIG. 9. Schematic four-level system.

over, the population-dependent amplitude and frequency of RO provide a detectable signature to the information that is stored in QD/QDM systems for a wide range of temperatures. This signature is useful in quantum information processing.

ACKNOWLEDGMENTS

The author would like to thank the National Science Council of Taiwan (Contract No. NSC95-2623-7-151-003-D) and the Ministry of Education for financially supporting this research.

[1]E. Knill, R. Laflamme, and G. Milburn, Nature (London) **409**, 46 (2001).
[2]G. Chen, N. H. Bonadeo, D. G. Steel, D. Gammon, D. S. Katzer, D. Park, and L. J. Sham, Science **289**, 1906 (2000).
[3]M. Bayer, P. Hawrylak, K. Hinzer, S. Fafard, M. Korkusinski, Z. R. Wasilewski, O. Stern, and A. Forchel, Science **291**, 451 (2001).
[4]W. Langbein, P. Borri, U. Woggon, V. Stavarache, D. Reuter, and A. D. Wieck, Phys. Rev. B **70**, 033301 (2004).
[5]P. Borri, W. Langbein, S. Schneider, U. Woggon, R. L. Sellin, D. Ouyang, and D. Bimberg, Phys. Rev. Lett. **87**, 157401 (2001).
[6]C. Bardot, M. Schwab, M. Bayer, S. Fafard, Z. Wasilewski, and P. Hawrylak, Phys. Rev. B **72**, 035314 (2005).
[7]G. Ortner, R. Oulton, H. Kurtze, M. Schwab, D. R. Yakovlev, M. Bayer, S. Fafard, Z. Wasilewski, and P. Hawrylak, Phys. Rev. B **71**, 125335 (2005).
[8]A. Zrenner, E. Beham, S. Stufler, F. Findeis, M. Bichler, and G. Abstreiter, Nature **418**, 612 (2002); H. Htoon, T. Takagahara, D. Kulik, O. Baklenov, A. L. Holmes, Jr., and C. K. Shih, Phys. Rev. Lett. **88**, 087401 (2002).
[9]E. A. Muljarov, T. Takagahara, and R. Zimmermann, Phys. Rev. Lett. **95**, 177405 (2005); A. Vagov, V. M. Axt, and T. Kuhn, Phys. Rev. B **67**, 115338 (2003); A. V. Uskov, A.-P. Jauho, B. Tromborg, J. Mork, and R. Lang, Phys. Rev. Lett. **85**, 1516 (2000).
[10]P. Borri, W. Langbein, U. Woggon, V. Stavarache, D. Reuter, and A. D. Wieck, Phys. Rev. B **71**, 115328 (2005); M. Bayer and A. Forchel, *ibid.* **65**, 041308 (2002).
[11]A. Vagov, V. M. Axt, T. Kuhn, W. Langbein, P. Borri, and U. Woggon, Phys. Rev. B **70**, 201305 (2004); A. Vagov, V. M. Axt, and T. Kuhn, *ibid.* **66**, 165312 (2002).
[12]S. Schmitt-Rink, D. A. B. Miller, and D. S. Chemla, Phys. Rev. B **35**, 8113 (1987).
[13]S. P. Mahanti and C. M. Varma, Phys. Rev. Lett. **25**, 1115 (1970).
[14]A. Lemaitre, A. D. Ashmore, J. J. Finley, D. J. Mowbray, M. S. Skolnick, M. Hopkinson, and T. F. Krauss, Phys. Rev. B **63**, 161309 (2001).
[15]R. Heitz, I. Mukhametzhanov, O. Stier, A. Madhukar, and D. Bimberg, Phys. Rev. Lett. **83**, 4654 (1999).
[16]M. Bissiri, G. B. Hoger von Hogersthal, A. S. Bhatti, M. Capizzi, A. Frova, P. Frigeri, and S. Franchi, Phys. Rev. B **62**, 4642 (2000).
[17]V. M. Fomin, V. N. Gladilin, J. T. Devreese, E. P. Pokatilov, S. N. Balaban, and S. N. Klimin, Phys. Rev. B **57**, 2415 (1998).
[18]S. Nomura and T. Kobayashi, Phys. Rev. B **45**, 1305 (1992).
[19]O. Verzelen, R. Ferreira, and G. Bastard, Phys. Rev. B **62**, R4809 (2000); O. Verzelen, R. Ferreira, and G. Bastard, *ibid.* **64**, 075315 (2001).
[20]S. Hameau, Y. Guldner, O. Verzelen, R. Ferreira, and G. Bastard, Phys. Rev. Lett. **83**, 4152 (1999), and references therein.
[21]M. Gurioli, A. Vinattieri, M. Zamfirescu, M. Colocci, S. Sanguinetti, and R. Notzel, Phys. Rev. B **73**, 085302 (2006).
[22]J. Feldmann, G. Peter, E. O. Gobel, P. Dawson, K. Moore, and C. Foxon, Phys. Rev. Lett. **59**, 2337 (1987).
[23]T. Inoshita and H. Sakaki, Phys. Rev. B **56**, R4355 (1997).
[24]E. Burstein, D. L. Mills, A. Pincruk, and S. Ushioda, Phys. Rev. Lett. **22**, 348 (1969).
[25]L. C. Andreani, G. Panzarini, and J.-M. Gerard, Phys. Rev. B **60**, 13276 (1999).
[26]E. Merzbacher, *Quantum Mechanics* (Wiley, New York, 1970).
[27]J. R. Schrieffer, *Theory of Superconductivity* (W. A. Benjamin, Reading, MA, 1964).
[28]N. Zettili, *Quantum Mechanics Concepts and Applications* (Wiley, New York, 2001).
[29]X.-Q. Li, H. Nakayama, and Y. Arakawa, Phys. Rev. B **59**, 5069 (1999).
[30]G. D. Mahan, *Many-Particle Physics* (Plenum, New York, 1981).
[31]C. Kittel, *Quantum Theory of Solids* (Wiley, New York, 1963).